

Philanthotoxin analogues that selectively inhibit ganglionic nicotinic acetylcholine receptors with exceptional potency

Hamid S Kachel,[†] Henrik Franzyk[‡] and Ian R Mellor^{†,*}

[†]School of Life Sciences, University of Nottingham, University Park, Nottingham, NG7 2RD, UK.

[‡]Department of Drug Design and Pharmacology, University of Copenhagen, Jagtvej 162, DK-2100 Copenhagen, Denmark.

Key words: nicotinic acetylcholine receptor; philanthotoxin; antagonism; open-channel block; *Xenopus* oocytes; two-electrode voltage clamp.

Abstract

Philanthotoxin-433 (PhTX-433) is an active component of the venom from the Egyptian digger wasp, *Philanthus triangulum*. PhTX-433 non-selectively inhibits several excitatory ligand-gated ion channels, and we recently showed that its synthetic analogue, PhTX-343, exhibits strong selectivity for neuronal over muscle-type nicotinic acetylcholine receptors (nAChRs). Here we examined the action of seventeen analogues of PhTX-343 against ganglionic ($\alpha 3\beta 4$) and brain ($\alpha 4\beta 2$) nAChRs expressed in *Xenopus* oocytes by using two-electrode voltage-clamp at -100 mV. IC_{50} values for PhTX-343 inhibition of $\alpha 3\beta 4$ and $\alpha 4\beta 2$ receptors were 7.7 nM and 80 nM, respectively. All of the studied analogues had significantly higher potency at $\alpha 3\beta 4$ nAChRs with IC_{50} values as low as 0.16 nM and with up to a 91-fold selectivity for $\alpha 3\beta 4$ over $\alpha 4\beta 2$ receptors. We conclude that PhTX-343 analogues displaying both a saturated ring and an aromatic moiety in the hydrophobic headgroup of the molecule demonstrate exceptional potency and selectivity for $\alpha 3\beta 4$ nAChRs.

Introduction

A constituent of the venom of the Egyptian digger wasp, *Philanthus triangulum*, is the polyamine-containing toxin, known as philanthotoxin-433 (PhTX-433; Fig. 1), which enables paralysis of its insect prey through inhibition of ionotropic glutamate receptors (iGluRs) and nicotinic acetylcholine receptors (nAChRs).^{1,2} The structure of PhTX-433 consists of a central tyrosine residue amide-linked to a thermospermine moiety on one side and to an *n*-butanoyl chain on the other (Fig. 1). The resulting molecule thus has a relatively bulky and hydrophobic ‘headgroup’ and a positively charged (+3) ‘tail’ at physiological pH. Although the wasp has evolved to produce toxins targeting iGluRs and nAChRs in insects, PhTX-433 and its structurally very similar synthetic analogue, PhTX-343 (**1**; Fig. 1), are also potent inhibitors of vertebrate ionotropic receptors. These latter interactions have been well characterized at mammalian iGluRs, including the *N*-methyl-D-aspartate (NMDA), kainate and α -amino-3-hydroxy-5-methyl-4-isoxazolepropionic acid (AMPA) receptors;^{3,4} as well as for vertebrate muscle-type^{5,6} and neuronal-type^{7,8} nAChRs. In our recent study on neuronal nAChRs, it was found that PhTX-343 is a very potent inhibitor of heteromeric receptors with selectivity for the ganglionic $\alpha 3\beta 4$ subtype.⁷

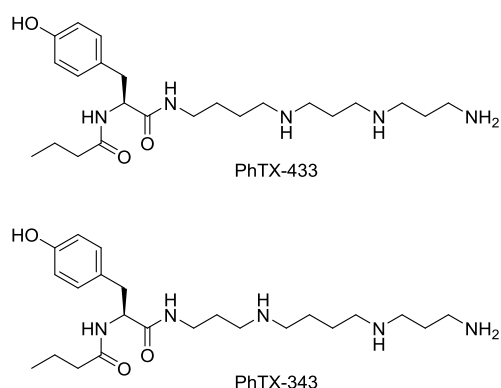


Figure 1. Structures of naturally occurring PhTX-433 and its synthetic analogue PhTX-343 (**1**), used as a template for the analogues studied in the present work.

Inhibition of both nAChRs and iGluRs by PhTX-343 has been shown to be use- and voltage-dependent (with increased inhibition occurring at more negative membrane potentials), and this has led to the hypothesis that open-channel blocking is the dominant mode of action, with the polyamine tail penetrating deep into the channel pore and interacting with polar amino acids, while the headgroup interacts with rings of hydrophobic amino acids at a more extracellular location in the pore.^{9, 10} Further evidence for this mechanism resulted from experiments showing that AMPA receptors lacking the GluA2 subunit are highly sensitive to PhTX-343, whereas those containing GluA2 are almost insensitive.¹¹ This can be explained by RNA editing of GluA2, resulting in a single amino acid substitution at the so-called “Q/R site” that forms the selectivity filter within the pore.⁹ Likewise, mutations in the outer pore of nAChR affect the affinity for PhTX-343.⁷

Studies into the importance of the amine functionalities resulted in the first breakthrough in receptor selectivity. Thus, the analogue PhTX-12, in which the two secondary amines in PhTX-343 were replaced with methylene groups, had an expected reduced potency at AMPA receptors and NMDA receptors, but unexpectedly inhibition of muscle-type nAChRs was significantly increased.⁴ However, the latter was accompanied by a change in the mode of action, since inhibition remained strong at positive membrane potentials and voltage dependence was weak.^{6, 10} In another study it was found that exchange of the tyrosine moiety in PhTX-343 for a cyclohexylalanine unit generated a toxin with considerably enhanced inhibitory activity at muscle-type nAChR.¹²

In the present work, we investigated PhTX-343 (**1**) and its headgroup-modified analogues (i.e., compounds **2-18**; Table 1) with single or combined structural alterations in the *n*-butanoyl, tyrosine and polyamine moieties for their inhibitory actions against the $\alpha 4\beta 2$ and $\alpha 3\beta 4$ subtypes of neuronal nAChRs. We aimed to develop analogues capable of distinguishing between neuronal heteromeric nAChR subtypes. Recently, there has been considerable interest in

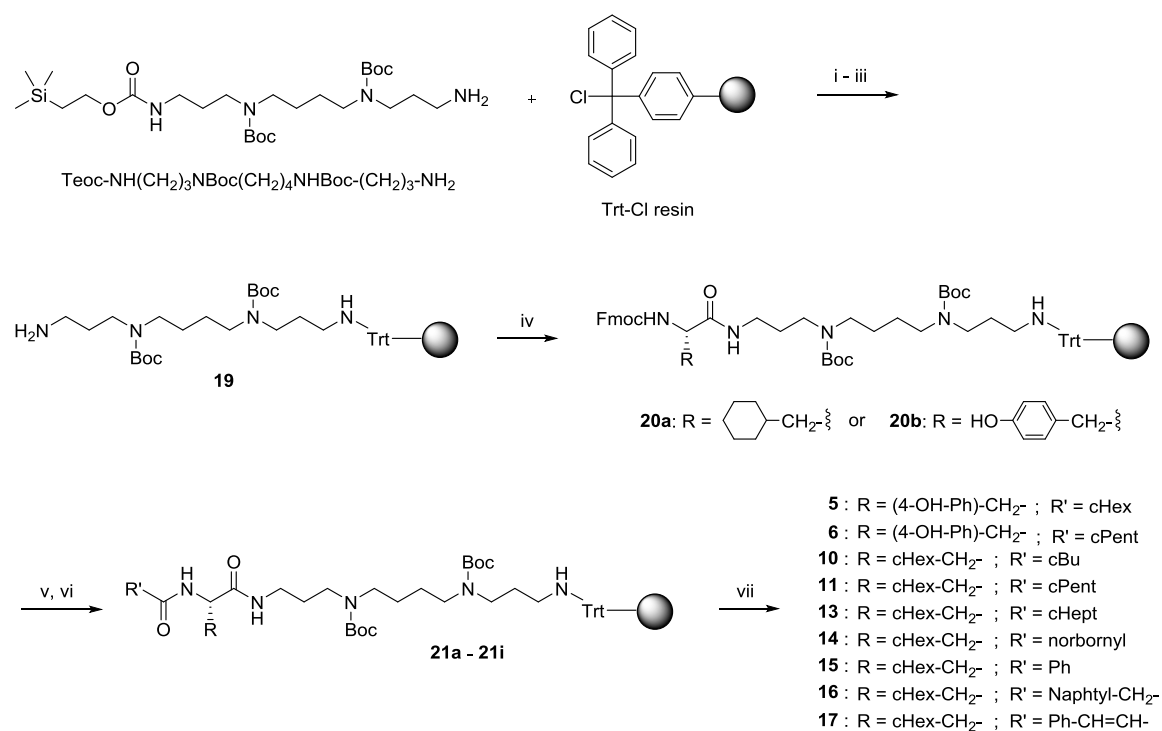
compounds that selectively inhibit the $\alpha 3\beta 4$ subtype of nAChRs as a potential treatment for nicotine addiction due to their significant expression in the medial habenula that modulates the mesolimbic dopaminergic response to nicotine.¹³ Hence, potent and selective $\alpha 3\beta 4$ nAChR antagonists have the potential to aid smoking cessation.^{14, 15}

Results

Synthesis of PhTX-343 analogues

The novel PhTX analogues **5**, **6**, **10**, **11**, and **13-17** were prepared by using a solid-phase synthesis (SPS) protocol similar to that reported previously for the known analogues **9**, **12**, and **18** displaying a cyclohexylalanine (Cha) residue.¹⁶ In brief, a large batch of trityl chloride polystyrene resin was loaded with an equimolar amount of mono-[2-(trimethylsilyl)ethyloxycarbonyl] (Teoc)-protected di-Boc-spermine (Scheme 1) in order to avoid the issue with cross-linking of the trityl linker moieties observed when employing di-Boc-spermine (i.e., $\text{H}_2\text{N}(\text{CH}_2)_3\text{NHBoc}(\text{CH}_2)_4\text{NHBoc}(\text{CH}_2)_3\text{NH}_2$).¹⁷ Next, unreacted trityl groups were capped with methanol in the presence of base (i.e., *i*Pr₂EtN in CH₂Cl₂), and subsequent removal of the Teoc N-protecting group by treatment with tetrabutylammonium fluoride afforded resin **19**. The prepared large batch of resin **19** was divided into several reactors to complete the last steps in the SPS of the individual analogues in parallel. This comprised acylation with the appropriate fluoren-9-yl-oxycarbonyl (Fmoc)-protected amino acid building blocks (i.e., Fmoc-Tyr(*t*Bu)-OH or Fmoc-Cha-OH) by standard diisopropylcarbodiimide (DIC)-1-hydroxybenzotriazol (HOBt) amide coupling to provide resins **20a** and **20b**, which then were Fmoc-deprotected and acylated with the selected different carboxylic acids under standard DIC-HOBt conditions. Subsequent cleavage (from resins **21a-21i**) and purification furnished PhTX analogues **5**, **6**, **10**, **11**, and **13-17** in 16% to 73% yield.

Scheme 1. Solid-phase synthesis of novel PhTX analogues.^a

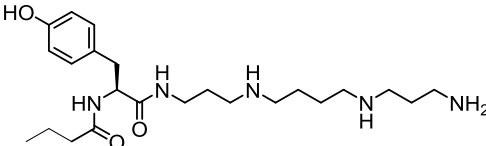
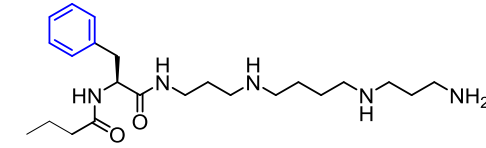
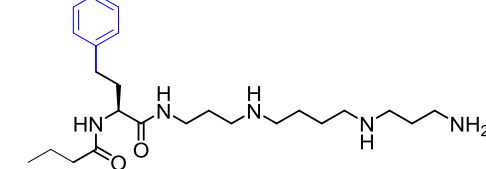
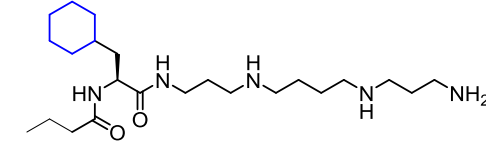
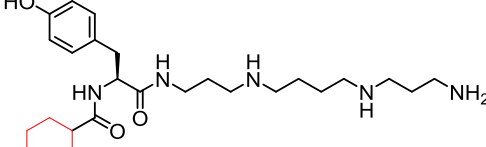
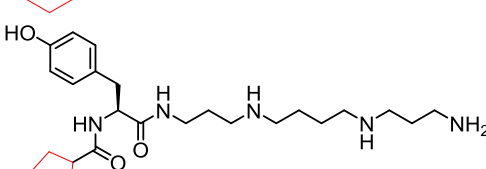
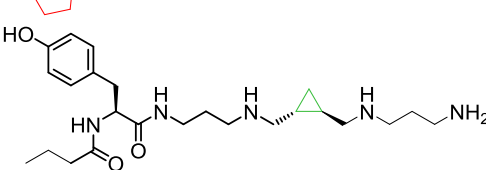
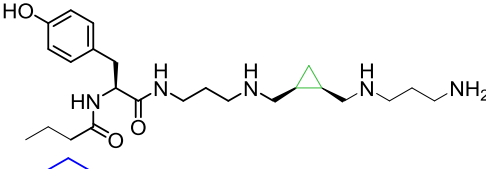
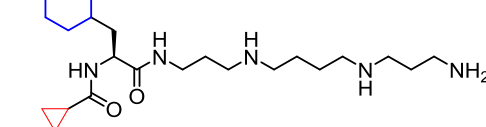


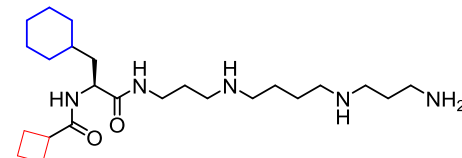
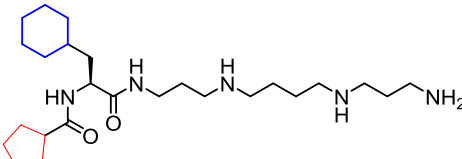
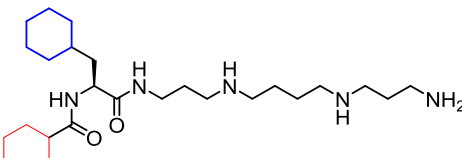
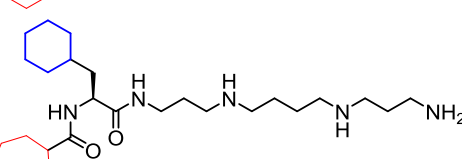
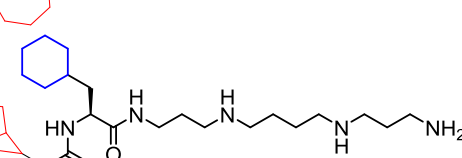
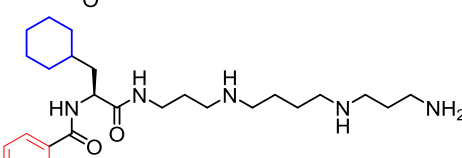
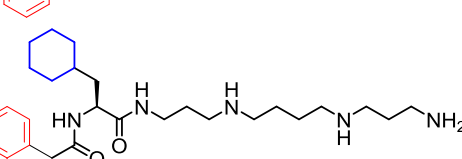
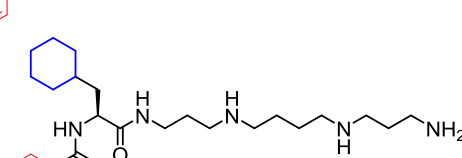
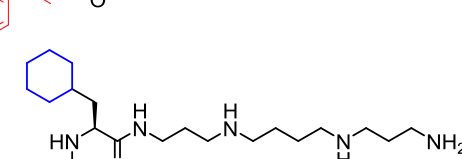
^a Reagents: (i) $i\text{Pr}_2\text{EtN}$ (3 equiv), CH_2Cl_2 , 3 days at room temperature; (ii) $i\text{Pr}_2\text{EtN-MeOH-CH}_2\text{Cl}_2$ (5:15:80, 2×15 min); (iii) Bu_4NF (4 equiv), DMF, 50°C , 1 h, then 1 h at room temperature; (iv) Fmoc-Cha-OH or Fmoc-Tyr(*t*Bu)-OH (3 equiv), DIC (3 equiv), HOBt (3 equiv), DMF, pre-activation for 20 min then 20 h after addition to resin; (v) 20% piperidine-DMF, 2×10 min; (vi) $\text{R}'\text{-COOH}$ (5 equiv), DIC (5 equiv), HOBt (5 equiv), DMF, 16 h; (vii) 50% TFA- CH_2Cl_2 , 2 h.

Our reference compound, PhTX-343 (**1**), had IC_{50} values of 7.7 nM and 80 nM at $\alpha 3\beta 4$ and $\alpha 4\beta 2$ receptors, respectively, thus displaying a ~ 10 -fold selectivity for the $\alpha 3\beta 4$ subtype over the $\alpha 4\beta 2$ subtype (Fig. 2; Table 1). Of the seventeen analogues (i.e., **2-18**) only one compound (i.e., **9**) was a less potent antagonist of the $\alpha 4\beta 2$ subtype, while all analogues were more efficient antagonists of the $\alpha 3\beta 4$ subtype (Fig. 3A-B). With respect to high selectivity for $\alpha 3\beta 4$ over $\alpha 4\beta 2$ receptors, two compounds (i.e., **5** and **16**) were identified as being particularly

promising (Fig. 3C). The results obtained for each subset of analogues, characterized by the number and type of structural modifications, are presented in more detail below.

Table 1. IC₅₀ values for inhibition of $\alpha 3\beta 4$ or $\alpha 4\beta 2$ receptors by compounds **1-18**.

Compound	$\alpha 3\beta 4$		$\alpha 4\beta 2$		Sel
	IC ₅₀ , nM (95% CI)	RP	IC ₅₀ , nM (95% CI)	RP	
	7.65 (6.31-9.28)	1.0	80.2 (48.5-132)	1.0	10.5
	0.93 (0.61-1.42)	8.2	27.8 (19.3-40.0)	2.9	29.9
	1.74 (1.17-2.60)	4.4	20.8 (14.5-29.9)	3.9	12.0
	2.62 (1.55-4.44)	2.9	2.58 (0.98-6.75)	31.1	1.0
	0.46 (0.35-0.61)	16.6	36.6 (28.6-46.8)	2.2	79.6
	0.57 (0.44-0.74)	13.4	22.5 (17.3-29.3)	3.6	39.5
	0.92 (0.69-1.23)	8.3	44.3 (36.3-54.2)	1.8	48.2
	1.44 (0.99-2.10)	5.3	47.4 (40.0-56.1)	1.7	32.9
	2.63 (2.12-3.28)	2.9	112 (80.4-155)	0.7	42.6

10		1.07 (0.80-1.45)	7.1	20.8 (9.12-47.4)	3.9	19.4
11		0.65 (0.40-1.06)	11.8	5.43 (2.99-9.86)	14.8	8.4
12		2.19 (1.55-3.11)	3.5	31.4 (20.3-48.4)	2.6	14.3
13		0.55 (0.44-0.70)	13.9	28.2 (19.1-41.5)	2.8	51.3
14		0.95 (0.64-1.39)	8.1	25.6 (16.8-39.2)	3.1	26.9
15		0.37 (0.22-0.64)	20.7	21.4 (14.2-32.3)	3.7	57.8
16		0.16 (0.11-0.23)	47.8	14.6 (11.0-19.4)	5.5	91.3
17		0.35 (0.28-0.43)	21.9	12.1 (8.47-17.4)	6.6	34.6
18		2.83 (1.51-5.30)	2.7	25.8 (17.4-38.4)	3.1	9.1

RP = relative potency as compared to that of **1** for the receptor subtype; Sel = selectivity of the compound for $\alpha 3\beta 4$ over $\alpha 4\beta 2$; 95% CI = 95% confidence interval; n = 4-20 oocytes.

Potency of analogues with substitution of tyrosine only

Three of the investigated analogues (**2-4**) contained alternative central amino acids instead of tyrosine (Tyr), thereby conferring increased hydrophobicity to the side chain (Table 1). Compounds **2** and **3** with a phenylalanine (Phe) moiety or its homologue (hPhe) instead of Tyr exhibited increased potency at both nAChR subtypes, which was more pronounced for $\alpha 3\beta 4$, thus leading to increased selectivities of 30-fold and 12-fold, respectively. Compound **4**, having a cyclohexylalanine (Cha) residue in place of Tyr, proved more potent than **1** at both nAChR subtypes, but noticeably all selectivity for $\alpha 3\beta 4$ over $\alpha 4\beta 2$ was abrogated (Fig. 2; Table 1). Interestingly, analogue **4** was the only compound tested in this study that showed this non-selective behaviour, while it was the most potent inhibitor of $\alpha 4\beta 2$ receptors (Fig. 2B).

Potency of analogues with alternative N-acyl moieties

In analogues **5-6**, the N-acyl moieties comprise cyclohexanoyl or cyclopentanoyl instead of the original N-butanoyl group, which confer increased bulk and hydrophobicity to the headgroup (Table 1). Analogues **5** and **6** showed a strong increase in potency at $\alpha 3\beta 4$ receptors, but less so at $\alpha 4\beta 2$ receptors, and hence selectivity for $\alpha 3\beta 4$ was increased up to 80-fold for compound **5**.

Potency of analogues with modifications in the polyamine tail moiety

Analogues **7** and **8** contain a cyclopropane ring in the centre of the polyamine moiety in a *trans* or *cis* conformation, respectively (Table 1). Both compounds exhibited moderately increased potency at $\alpha 3\beta 4$ receptors as compared to that of **1**, whereas they only displayed weakly improved inhibition of $\alpha 4\beta 2$ receptors. This gave rise to increased selectivity of **7** and **8** for $\alpha 3\beta 4$ receptors to 48-fold and 33-fold, respectively.

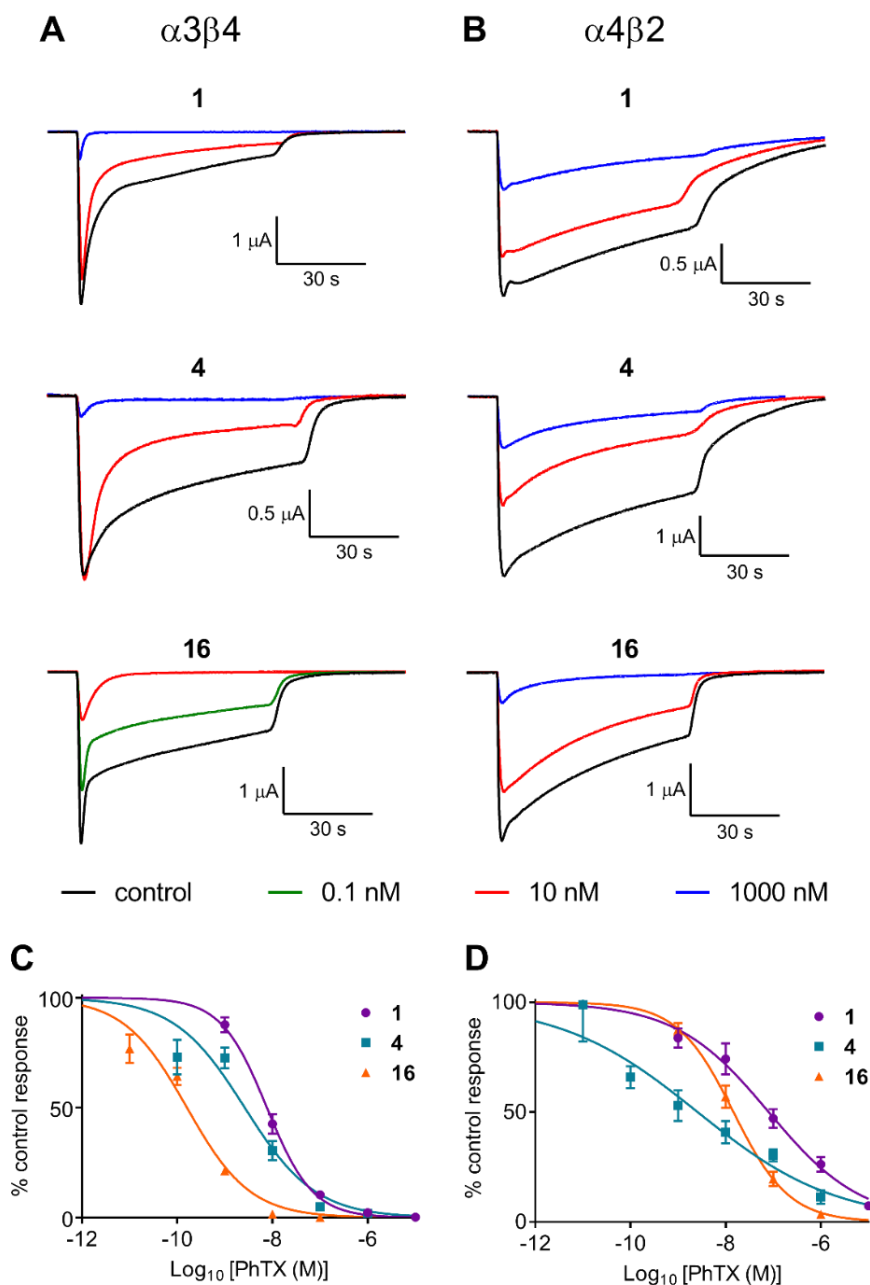


Figure 2. Inhibition of nAChR responses by PhTX-343 analogues. **A-B:** Two-electrode voltage clamp (TEVC) current responses of $\alpha 3\beta 4$ (**A**) or $\alpha 4\beta 2$ (**B**) nAChRs to 100 μM or 10 μM ACh respectively, in the absence and co-applied with compounds **1**, **4** or **16**. **C-D:** Concentration-inhibition curves for inhibition of $\alpha 3\beta 4$ (**C**) or $\alpha 4\beta 2$ (**D**) nAChRs by compounds **1**, **4** or **16**. Data points are represented as mean \pm SEM ($n = 3-9$), and curves were obtained via fitting to Eq. 1 (see experimental section on data analysis). IC_{50} values are given in Table 1.

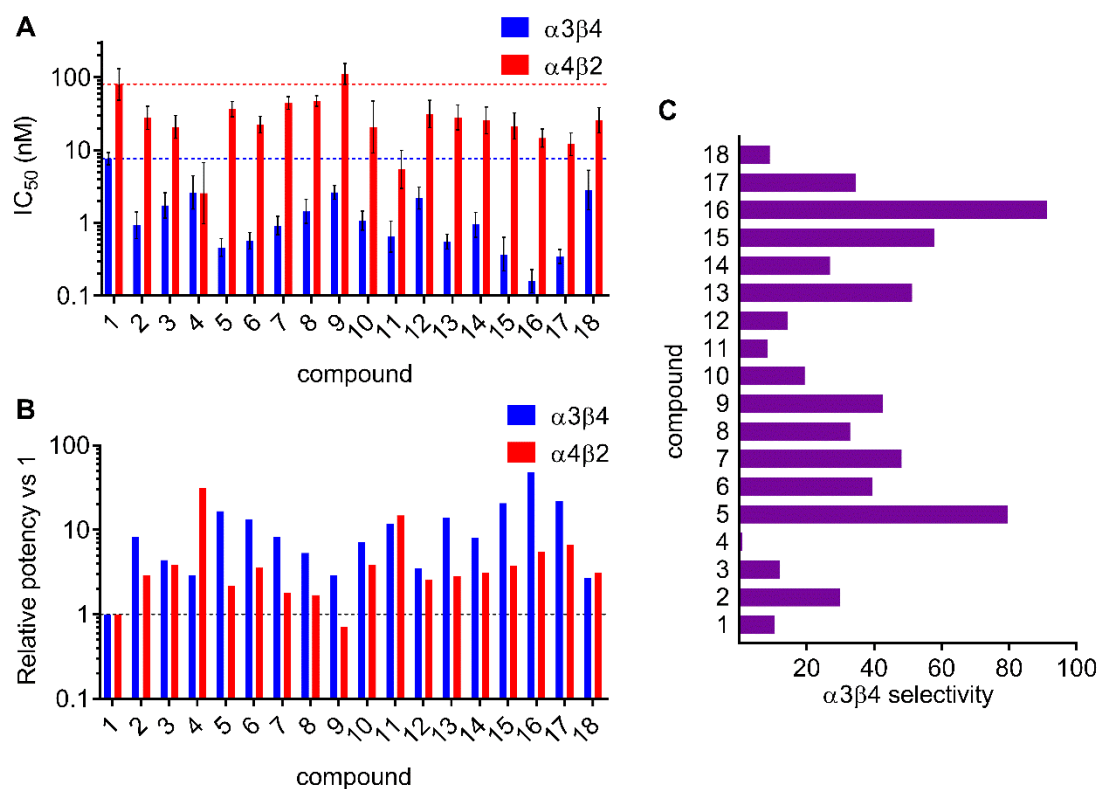


Figure 3. Summary of potency and selectivity of inhibition of $\alpha 3\beta 4$ and $\alpha 4\beta 2$ nAChR subtypes by compounds **1-18**. **A:** IC₅₀ values for inhibition of $\alpha 3\beta 4$ (blue bars) or $\alpha 4\beta 2$ (red bars). Error bars indicate 95% CI. **B:** Relative potency as compared to that of **1** (i.e., PhTX-343) for each nAChR subtype ($\alpha 3\beta 4$ - blue bars; $\alpha 4\beta 2$ - red bars). **C:** Selectivity for the $\alpha 3\beta 4$ subtype.

Potency of analogues with a combination of two headgroup modifications

This set of ten compounds all contain a Tyr \rightarrow Cha substitution. The effect of this change alone can be seen in the inhibitory profile of analogue **4**, for which no selectivity for $\alpha 3\beta 4$ over $\alpha 4\beta 2$ was found. Six of the compounds (i.e., **9-14**), containing small to large saturated ring systems instead of the *n*-butanoyl moiety (Table 1), showed minor to moderately increased potency at $\alpha 3\beta 4$ receptors, while displaying reduced to moderately increased potency at $\alpha 4\beta 2$ receptors, except for analogue **11** that was a 15-fold more potent inhibitor than **1** at the latter receptor. Selectivity for $\alpha 3\beta 4$ was variable within this series of six compounds with **11** having slightly

reduced selectivity as compared to that of **1**, while **9** and **13** proved to be considerably more selective (43-fold and 51-fold, respectively) than the original lead compound (i.e., **1**).

The remaining four compounds in this subclass (i.e., **15-18**) all have aromatic N-acyl substituents (Table 1). Except for **18**, containing an extended and rigid biphenyl group, the introduction of aromatic moieties resulted in very strongly increased inhibitory potency (as compared to that of **1**) at $\alpha 3\beta 4$ receptors. By contrast, only weak to moderate enhancement of potency at $\alpha 4\beta 2$ was observed for these analogues, resulting in a highly improved selectivity for $\alpha 3\beta 4$. In fact, compound **16**, carrying a naphthoyl group proved to be the most potent and selective among all the analogues tested in the present study, as it was 48-fold more potent than **1** at $\alpha 3\beta 4$ (i.e., with an $IC_{50} = 0.16$ nM) combined with a selectivity of 91-fold in favour of $\alpha 3\beta 4$ (Fig. 2 and 3).

Discussion and Conclusion

In the present work it was demonstrated that analogues of PhTX-343 (**1**) can be designed to exhibit extremely high antagonistic potency at nAChR receptors, and in particular at the $\alpha 3\beta 4$ subtype. The most potent analogue was **16**, containing an N-naphthoyl-Cha headgroup and a spermine polyamine tail, with an IC_{50} of 0.16 nM. This is certainly the most potent known PhTX-343-derived antagonist of nAChR, and to our knowledge it is the most potent nAChR antagonist reported to date. Additionally, compound **16** has high selectivity for $\alpha 3\beta 4$ over $\alpha 4\beta 2$, and based on our recent observations that PhTX-343 selectively inhibits $\beta 4$ -containing nAChRs (especially $\alpha 3\beta 4$) over all of the other major nAChR subtypes (i.e., $\alpha 4\beta 2$, $\alpha 3\beta 2$, $\alpha 7$ and $\alpha 1\beta 1\gamma\delta$)⁷ it is expected that this will be the case also for **16**. Many of the compounds described in the present work also compare favourably to a recently identified synthetic α -conotoxin, TP-2212-59, that selectively targets $\alpha 3\beta 4$ nAChRs with a low nanomolar IC_{50} value (2.3 nM).¹⁸ However, a direct comparison between compounds belonging to these two distinct

classes of antagonists are not straightforward due to their different binding sites and mode of action.

The proposed binding site for PhTX-343 and its analogues, having similar highly charged polyamine tail regions, is located within the nAChR pore, whereby the polyamine moiety inserts deeply into the pore in order to interact with the threonine and serine rings beyond the equatorial leucine gate, while the bulky and hydrophobic headgroup interacts with hydrophobic residues of the valine and leucine rings that line the outer part of the pore.¹⁰

Compound **16** possesses modifications in both the N-acyl and the central amino acid residue, and it may thus be considered to be a further modification of PhTX(Cha)-343 (**4**), which previously was identified as an antagonist of human muscle nAChRs in TE671 cells, where it proved 277-fold more potent than **1** at $V_H = -100$ mV.¹² Nevertheless, in the present study, by using the same holding potential, only a 2.9-fold increase in relative potency of **4** (versus that of **1**) at $\alpha 3\beta 4$ was found, most likely arising from the fact that **1** is much more potent (317-fold) at $\alpha 3\beta 4$ than at the $\alpha 1\beta 1\gamma\delta$ subtype.⁷

Interestingly, the four most potent analogues at $\alpha 3\beta 4$ receptors, having IC_{50} values < 0.5 nM (i.e., **5**, **15**, **16** and **17**), all shared the structural characteristic of a more bulky and hydrophobic headgroup, consisting of a saturated aliphatic ring and an aromatic group. A putative explanation for this relates to our understanding of why PhTX-343 is selective for $\beta 4$ -containing nAChRs.⁷ Earlier it was proposed that the $\alpha 3\beta 4$ selectivity arises from the presence of a phenylalanine residue (F275; in the rat receptor) uniquely found at the valine ring in $\beta 4$ subunits.⁷ This Phe promotes aromatic stacking interactions and greatly increases affinity of appropriately substituted ligands, which also may provide a rationale as to why **5**, **6**, **15**, **16** and **17** display enhanced selectivity for $\alpha 3\beta 4$ over $\alpha 4\beta 2$. Based on this hypothesis, compound **18** might also be expected to be a highly potent and selective inhibitor of $\alpha 3\beta 4$ receptors, however,

its aromatic moiety is quite extended and rigid, which may restrict access to its binding position due to steric hindrance.

Other highly potent compounds comprise **11**, **13** and **14** that have a Tyr → Cha substitution and a bulky saturated hydrophobic aliphatic ring structure instead of the linear *n*-butanoyl moiety. This increases headgroup hydrophobicity considerably, and it is beneficial for interaction with valine and leucine residues in the outer pore regions of both nAChR subtypes. Furthermore, compounds **2** and **7** also had sub-nanomolar IC₅₀ values, and **2** was previously found to have increased potency at *Torpedo* electric organ nAChRs through testing in a [³H]H₁₂-HTX binding assay,¹⁹ presumably because of an increased headgroup hydrophobicity induced by the Tyr → Phe substitution resulting in the absence of a hydroxyl group. Compound **7** has a cyclopropane functionality inserted into the centre of the spermine moiety, and previous modelling studies indicate that internal hydrogen bonding between the amine closest to the headgroup and the amide oxygens will position the cyclopropane unit so that it contributes to the bulkiness of the headgroup.^{10, 20}

At $\alpha 4\beta 2$ receptors analogue **4** was the most potent antagonist, whereas it was one of the least potent compounds at $\alpha 3\beta 4$ receptors. This most likely arises from the absence of an aromatic moiety in the headgroup, providing improved hydrophobic interactions with the valine and leucine residues in the outer pore region of $\alpha 4\beta 2$ than any of the other compounds. The second most potent compound (i.e., **11**) at $\alpha 4\beta 2$ also lacked an aromatic group, however, other non-aromatic compounds had lower potency, presumably due to lack of optimal shape and/or size restrictions.

In summary, PhTX-343 analogues displaying both a saturated ring structure and an aromatic moiety in the headgroup demonstrate extreme potency and selectivity for the $\alpha 3\beta 4$ nAChR subtype, and it is hypothesised that this arises from the unique presence of a Phe residue in the outer pore region of this receptor subtype. The most selective compounds identified may have

potential as smoking cessation therapies and find application as useful probes in the study of nicotine addiction.

Experimental Section

Materials. Starting materials (amino acid building blocks, trityl chloride polystyrene resin, and reagents) and solvents were obtained from commercial suppliers (Iris Biotech, Sigma-Aldrich, VWR, Labscan and CHEMsolute) and used as received. CH₂Cl₂ was distilled from P₂O₅ and stored over 4 Å molecular sieves.

Acetylcholine (ACh) was from Sigma. PhTX-343 (**1**) was synthesized as described in Wellendorph et al.²¹ Some analogues have been synthesized previously: Compounds **2** and **3**;²² compound **4**,¹² compounds **7** and **8**,²⁰ as well as compounds **9**, **12**, and **18**.¹⁶ cDNA clones of rat neuronal nAChR subunits (α 3, α 4, β 2 and β 4) were from the Salk Institute for Biological Studies (Professor Stephen Heinemann). Plasmids were linearized and cRNA transcribed using an mMessage mMachine kit (Ambion).

General Methods for Purification and Compound Characterization. Solid-phase conversions were carried out in Teflon filter vessels on a Scansys PLS 4 × 6 Organic Synthesizer equipped with a heating block. Water used during analytical and preparative HPLC was filtered through a 0.22 µm membrane filter. Preparative HPLC was performed by using a Luna C18(2) column (250 mm × 21.2 mm; particle size: 5 µm) on an Agilent 1100 LC system consisting of two preparative pump units and equipped with a multiple-wavelength UV detector. Linear gradients for elution were composed by mixing solvent A (MeCN–H₂O–TFA 5:95:0.1) and B (MeCN–H₂O–TFA 95:5:0.1) at a flow rate of 20 mL/min; injection volumes were 300-900 µL. Analytical HPLC was performed on a Shimadzu system comprising an SCL-10A VP controller, an SIL-10AD VP autosampler, an LC-10AT VP pump, an SPD-M10A VP diode array detector, and a CTO-10AC VP column oven, using a Phenomenex Luna C18(2)

column (150 × 4.6 mm; particle size: 3 μm). The HPLC system was controlled by Class VP 6 software; elution with a flow of 0.8 mL/minute; injection volumes were 5-10 μL of ~1 mg/mL solutions, and separations were performed at 40 °C. The same eluents as for preparative HPLC (i.e., A = MeCN–H₂O–TFA 5:95:0.1 and B = MeCN–H₂O–TFA 95:5:0.1) were used. The purities of target compounds **5**, **6**, **10**, **11** and **13-17** (as determined from UV absorption integration at λ = 210 nm or 220 nm) were at least 95%. ¹H and ¹³C nuclear magnetic resonance (NMR) spectra were acquired on a 600 MHz Bruker Avance III HD spectrometer equipped with a cryogenically cooled 5 mm dual probe optimized for ¹H and ¹³C. Samples were dissolved in methanol-d₄ (Cambridge Isotope Laboratories), and was then analyzed at 300 K using the residual solvent peak internal standard (i.e., δ_C = 49.00 ppm and δ_H = 3.31 ppm). Coupling constants (*J* values) are given in hertz (Hz), and multiplicities of ¹H NMR signals are reported as follows: singlet (s), doublet (d), doublet of doublets (dd), triplet (t), pentet (p), multiplet (m); broadened (br). Additional peaks due to the presence of rotamers or presence of chiral centers are designated by an asterisk (*); two close signals with almost the same chemical shift value is indicated by two asterisks (**). Numbering of carbon atoms: polyamine is numbered 1, 2, 3 etc starting from the amide terminus; amino acid moiety is numbered α, β, γ etc; the N-acyl moiety is numbered 1', 2', 3' etc. High-resolution MALDI-TOF spectra were obtained on a Bruker Solarix XR in MALDI mode giving (m/z): [M + H]⁺ with ΔM below 2 ppm.

Synthesis of philanthotoxin analogues. The novel PhTX analogues **5**, **6**, **10**, **11**, and **13-17** were prepared in a similar manner to that reported previously.¹⁶ In brief, trityl chloride polystyrene resin (1.66 g, 2.2 mmol/g) in a syringe (20 mL, fitted with a polypropylene filter and a Teflon valve), was swelled in dry CH₂Cl₂ and then treated with 10% iPr₂EtN–CH₂Cl₂ (10 mL) for 5 min, and finally washed with CH₂Cl₂ (2 × 10 mL; each for 5 min). Then H₂N(CH₂)₃-NBoc(CH₂)₄NBoc(CH₂)₃NHTeoc²¹ (2.00 g, 3.65 mmol) and iPr₂EtN (1.9 mL, 3 × 3.65 mmol) in CH₂Cl₂ (25 mL) was added to the resin in a round-bottomed flask (50 mL). After

gentle stirring for 3 days, the resin was transferred to a syringe (20 mL), washed with CH₂Cl₂ (2 × 15 mL, each for 5 min), and capped with iPr₂EtN–MeOH–CH₂Cl₂ (5:15:80, 2 × 15 mL, each for 15 min). Upon draining, the resin was washed with CH₂Cl₂, DMF, and CH₂Cl₂ (each 3 ×), and then transferred to a round-bottomed flask (100 mL), in which Teoc deprotection was performed with Bu₄NF (3 equiv) in dry DMF (50 mL) for 1 h at 50 °C followed by 1 h at room temperature. The resin was transferred to a syringe followed by draining and washing with DMF, MeOH, DMF, and CH₂Cl₂ (each 3 ×) and finally dried for 16 h to yield resin-bound spermine (2.93 g, ~1.2 mmol/g). Portions of the resin (0.120 g, ~0.15 mmol) were placed in Teflon filter vessels, and were then preswollen in dry DMF (5 mL). A mixture of Fmoc-Cha-OH (3 equiv) or Fmoc-Tyr(*t*Bu)-OH (3 equiv), DIC (3 equiv), and HOBt (3 equiv) in dry DMF (3 mL/reactor) was stirred for 20 min, filtered, and added (ca. 3 mL) to each of the resins in the filter vessels, which were shaken for 20 h, drained and washed with DMF, MeOH, DMF, and CH₂Cl₂ (each 3 ×), and then Fmoc-deprotected with 20% piperidine–DMF (3 mL, 2 × 10 min). Following wash with DMF (5 ×), a preincubated (for 15 min) mixture of the appropriate carboxylic acid (5 equiv), HOBt (5 equiv), and DIC (5 equiv) in dry DMF (3 mL) was added to the respective reactors, which then were shaken at room temperature for 16 h. The resins were then drained and washed with DMF, MeOH, DMF, and CH₂Cl₂ (each 3 ×). Cleavage of the products from the resin was performed with 50% TFA–CH₂Cl₂ (5 mL for 2 h). The resins were further eluted with CH₂Cl₂ and MeOH (each 2 × 5 mL); the total eluates from each reactor were co-evaporated with toluene–MeOH 1:1 (3 × 10 mL). The resulting crude products were dried overnight, and then purified by preparative HPLC (by using a linear gradient rising from 5% B to 100% B during 20 min) to give PhTX analogues **5**, **6**, **10**, **11**, and **13-17** as the tris(TFA) salts. Compounds **10** and **11** required rechromatography (using a linear gradient from 5% B to 60% B during 20 min) to obtain samples with sufficient purity.

PhTX analogue 5 (5): Yield: 58 mg (47%); $t_R = 18.56$ min. HRMS: calcd for $C_{26}H_{45}N_5O_3$ $[M + H]^+$ 476.3601, found 476.3600. 1H NMR (600 MHz, CD_3OD): δ 7.05 (2H, d, $J = 8.5$ Hz, H-b/H-b'), 6.71 (2H, d, $J = 8.5$ Hz, H-c/H-c'), 4.38 (1H, t, $J = 7.8$ Hz, H- α), 3.29-3.17 (2H, br m, H-1), 3.16-3.13 (2H, m - CH_2 -NH-) and 3.11-3.04 (4H, m, - CH_2 -NH-), 3.02-2.94 (3H, m, H_A - β and - CH_2 -NH-), 2.91-2.82 (3H, br m, H_B - β and - CH_2 -NH-), 2.22 (1H, m, H-2'), 2.09 (2H, m, H-9), 1.84-1.72 (9H, br m, H-2, H-5, H-6, $3 \times cHex$ - H_{eq}), 1.70-1.65 (2H, $cHex$ - H_{eq}), 1.40-1.16 (5H, br m, $cHex$ - H_{ax}). ^{13}C NMR (150 MHz, CD_3OD): δ 179.2, 175.2, 157.4, 131.3 (2C), 128.9, 116.3 (2C), 56.9, 48.3, 48.2, 46.2, 45.9 (2C), 37.9, 37.8, 36.7, 30.8, 30.3, 27.4, 26.9, 26.8, 26.6, 25.4, 24.3, 24.2.

PhTX analogue 6 (6): Yield: 88 mg (73%); $t_R = 16.98$ min. HRMS: calcd for $C_{25}H_{43}N_5O_3$ $[M + H]^+$ 462.3444, found 462.3444. 1H NMR (600 MHz, CD_3OD): δ 7.05 (2H, d, $J = 8.5$ Hz, H-b/H-b'), 6.72 (2H, d, $J = 8.5$ Hz, H-c/H-c'), 4.37 (1H, t, $J = 7.7$ Hz, H- α), 3.26 and 3.20 (each 1H, m, H-1), 3.16-3.12 (2H, m - CH_2 -NH-) and 3.10-3.04 (4H, m, - CH_2 -NH-), 3.01-2.95 (3H, m, H_A - β and - CH_2 -NH-), 2.91-2.82 (3H, br m, H_B - β and - CH_2 -NH-), 2.67 (1H, m, H-2'), 2.09 (2H, m, H-9), 1.85-1.75 (8H, br m, H-2, H-5, H-6, and $2 \times cPent$ -H), 1.71-1.63 (3H, br m, $cPent$ -H), 1.62-1.50 (3H, br m, $cPent$ -H). ^{13}C NMR (150 MHz, CD_3OD): δ 179.3, 175.2, 157.4, 131.3 (2C), 128.9, 116.3 (2C), 57.0, 48.3, 48.2, 46.2, 46.0, 45.9, 38.0, 37.8, 36.7, 31.8, 31.0, 27.4, 27.0, 26.9, 25.4, 24.3, 24.2.

PhTX analogue 10 (10): Yield: 23 mg (20%) and a fraction of almost pure **10** (25 mg); $t_R = 15.45$ min. HRMS: calcd for $C_{24}H_{47}N_5O$ $[M + H]^+$ 438.3803, found 438.3800. 1H NMR (600 MHz, CD_3OD): δ 4.23 (1H, br t, $J = 7.7$ Hz, H- α), 3.35 and 3.27 (each 1H, m, H-1), 3.22 (1H, p, $J = 8.5$ Hz, H-2'), 3.14 (2H, m, - CH_2 -NH-), 3.10-2.99 (8H, br m, $4 \times$ - CH_2 -NH-), 2.26 (1H, m, $cBut$ -H), 2.22-2.16 (2H, br m, $cBut$ -H), 2.15-2.06 (3H, br m, H-9, $cBut$ -H), 2.00 (1H, m, $cBut$ -H), 1.90-1.83 (3H, H-2 and $cBut$ -H), 1.80 (4H, m, H-5 and H-6), 1.78-1.70 (4H, br m, $cHex$ - H_{eq}), 1.67 (1H, m, $cHex$ - H_{eq}), 1.57 (2H, br t, $J = 7.4$ Hz, H- β), 1.35 (1H, m, H- γ), 1.30-

1.15 (3H, br m, cHex-H_{ax}), 1.01-0.79 (2H, br m, cHex-H_{ax}). ¹³C NMR (150 MHz, CD₃OD): δ 178.1, 176.8, 53.1, 48.3, 48.2, 46.2, 45.9, 40.4, 40.2, 37.8, 36.7, 35.5, 34.8, 33.3, 27.6, 27.5, 27.4, 27.2, 26.5, 25.7, 25.4, 24.3 (2C), 19.1.

PhTX analogue 11 (11): Yield: 19 mg (16%) and a fraction of almost pure **11** (21 mg); t_R = 16.91 min. HRMS: calcd for C₂₅H₄₉O₂N₅ [M + H]⁺ 452.3959, found 452.3958. ¹H NMR (600 MHz, CD₃OD): δ 4.24 (1H, dd, *J* = 9.3 and 6.0 Hz, H-α), 3.35 and 3.28 (each 1H, m, H-1), 3.13 (2H, br t, *J* = 7.8 Hz, -CH₂-NH-), 3.10-2.99 (8H, br m, 4 × -CH₂-NH-), 2.74 (1H, p, *J* = 7.9 Hz, H-2'), 2.08 (2H, m, H-9), 1.94-1.78 (8H, H-2, H-5, H-6 and 2 × cPent-H), 1.77-1.65 (9H, 4 × cPent-H and 5 × cHex-H_{eq}), 1.64-1.54 (4H, 2 × cPent-H and H-β), 1.37 (1H, m, H-γ), 1.32-1.15 (3H, br m, cHex-H_{ax}), 1.02-0.80 (2H, br m, cHex-H_{ax}). ¹³C NMR (150 MHz, CD₃OD): δ 179.7, 176.8, 53.2, 48.3, 48.2, 46.2, 46.0, 45.9, 40.2, 37.8, 36.7, 35.5, 34.8, 33.3, 32.0, 31.0, 27.6, 27.5, 27.4, 27.2, 27.1, 27.0, 25.4, 24.3 (2C).

PhTX analogue 13 (13): Yield: 50 mg (40%); t_R = 18.67 min. HRMS: calcd for C₂₇H₅₄N₅O₂ [M + H]⁺ 480.4272, found 480.4272. ¹H NMR (600 MHz, CD₃OD): δ 4.21 (1H, dd, *J* = 9.7 and 5.6 Hz, H-α), 3.35 and 3.27 (each 1H, m, H-1), 3.13 (2H, br t, *J* = 7.7 Hz, -CH₂-NH-), 3.10-2.99 (8H, br m, 4 × -CH₂-NH-), 2.45 (1H, m, H-2'), 2.09 (2H, m, H-9), 1.89-1.71 (14H, m, H-2, H-5, H-6, 4 × cHex-H_{eq}, 4 × cHep-H), 1.70-1.46 (11H, cHex H_{eq}, 8 × cHep-H, H-β), 1.37 (1H, m, H-γ), 1.34-1.15 (3H, br m, cHex-H_{ax}), 1.02-0.87 (2H, br m, cHex-H_{ax}). ¹³C NMR (150 MHz, CD₃OD): δ 180.7, 176.8, 53.0, 48.3, 48.2, 47.5, 46.2, 45.9, 40.2, 37.8, 36.7, 35.5, 34.8, 33.3, 33.1, 32.3, 29.3, 29.1, 27.8 (2C), 27.6, 27.5, 27.4, 27.2, 25.4, 24.3 (2C).

PhTX analogue 14 (14): Yield: 56 mg (45%); t_R = 19.17 min. HRMS: calcd for C₂₈H₅₄N₅O₂ [M + H]⁺ 492.4273, found 492.4271. ¹H NMR (600 MHz, CD₃OD): δ 4.26 (1H, dd, *J* = 8.9 and 5.5 Hz, H-α), 3.34 and 3.29 (each 1H, m, H-1), 3.13 (2H, br t, *J* = 7.8 Hz, -CH₂-NH-), 3.10-2.99 (8H, br m, 4 × -CH₂-NH-), 2.25-1.95 (6H, H-2', H-9 and 2 × Norbornyl-H), 1.91-1.66 (12H, H-2, H-5, H-6, 5 × cHex-H_{eq}, Norbornyl-H), 1.62-1.36 (7H, H-β, H-γ, 4 ×

Norbornyl-H), 1.35-1.08 (7H, 4 × Norbornyl-H, 3 × cHex-H_{ax}), 1.02-0.87 (2H, br m, cHex-H_{ax}). ¹³C NMR (150 MHz, CD₃OD): δ 176.6*, 175.9*, 53.0*, 48.3, 48.2, 46.2, 45.9, 43.7*, 42.3**, 42.2**, 40.7**, 40.5**, 40.1**, 40.0**, 38.6, 38.0*, 37.8, 36.7, 36.0**, 35.9**, 35.5**, 35.4**, 34.9, 33.1*, 30.9**, 30.8**, 29.6*, 27.6**, 27.5**, 27.4*, 27.2, 25.4, 24.3 (2C); * two close peaks arising from two rotamers or the presence of an additional chiral center; ** peak splitting due to presence of two rotamers the presence of an additional chiral center.

PhTX analogue 15 (15): Yield: 55 mg (46%); t_R = 17.11 min. HRMS: calcd for C₂₆H₄₆N₅O₂ [M + H]⁺ 460.3646, found 460.3645. ¹H NMR (600 MHz, CD₃OD): δ 7.88 (2H, br d, *J* = 8.5 Hz, H-2' and H-6'), 7.57 (1H, br t, *J* = 8.5 Hz, H-4'), 7.49 (2H, br t, *J* = 7.7 Hz, H-3' and H-5'), 4.48 (1H, dd, *J* = 10.0 and 5.3 Hz, H-α), 3.42 and 3.29 (each 1H, m, H-1), 3.11-2.98 (10H, br m, H-3, H-4, H-7, H-8 and H-10), 2.07 (2H, br p, *J* = 7.5 Hz, H-9), 1.90 (1H, m, H-2), 1.85-1.72 (9H, br m, H-5, H-6, 4 × cHex-H_{eq} and H_A-β), 1.70-1.65 (2H, br m, H_B-β and cHex-H_{eq}), 1.34-1.17 (3H, br m, cHex-H_{ax}), 1.06-0.94 (2H, br m, cHex-H_{ax}). ¹³C NMR (150 MHz, CD₃OD): δ 176.8, 170.7, 135.1, 133.1, 129.6 (2C), 128.6 (2C), 54.0, 48.2, 48.1, 46.1, 45.9, 40.0, 37.8, 36.7, 35.7, 34.8, 33.5, 27.6, 27.5, 27.4, 27.2, 25.4, 24.2 (2C).

PhTX analogue 16 (16): Yield: 54 mg (42%); t_R = 20.60 min. HRMS: calcd for C₃₁H₅₀N₅O₂ [M + H]⁺ 524.3965, found 524.3957. ¹H NMR (600 MHz, CD₃OD): δ 8.08 (1H, br d, *J* = 7.6 Hz, Ar-H), 7.90 (1H, br d, *J* = 7.6 Hz, Ar-H), 7.83 (1H, m, Ar-H), 7.56-7.50 (2H, br m, Ar-H), 7.47-7.45 (2H, br m, Ar-H), 4.24 (1H, dd, *J* = 10.5 and 5.5 Hz, H-α), 4.10 and 4.06 (each 1H, d, *J* = 15.5 Hz, H-2'), 3.35 and 3.23 (each 1H, m, H-1), 3.10-2.98 (4H, m, H-8 and H-10), 2.97 (2H, m, H-4/H-7), 2.83 (2H, t, *J* = 7.2 Hz, H-3), 2.74 (2H, m, H-4/H-7), 2.06 (2H, br p, *J* = 7.7 Hz, H-9), 1.80 (2H, br p, *J* = 6.7 Hz, H-2), 1.72-1.53 (11H, br m, H-5, H-6, H-β, cHex-H_{eq}), 1.27 (1H, m, H-γ), 1.24-1.03 (3H, br m, cHex-H_{ax}), 0.97-0.81 (2H, br m, cHex-H_{ax}). ¹³C NMR (150 MHz, CD₃OD): δ 176.4, 174.4, 135.4, 133.6, 133.1, 129.8, 129.2, 129.0, 127.4, 126.9,

126.7, 125.1, 53.5, 48.2, 47.9, 46.0, 45.8, 41.0, 40.0, 37.8, 36.7, 35.3, 34.9, 33.2, 27.5 (2C), 27.3, 27.1, 25.4, 24.2, 24.1.

PhTX analogue 17 (17): Yield: 51 mg (41%); $t_R = 20.01$ min. HRMS: calcd for $C_{28}H_{48}N_5O_2$ $[M + H]^+$ 486.3803, found 486.3802. 1H NMR (600 MHz, CD_3OD): δ 7.58 (2H, dd, $J = 8.0$ and 1.4 Hz, H-2' and H-6'), 7.55 (1H, d, $J = 15.8$ Hz, H- β'), 7.43-7.38 (3H, br m, H-3', H-4', H-5'), 6.74 (1H, d, $J = 15.8$ Hz, H- α'), 4.38 (1H, dd, $J = 9.1$ and 6.0 Hz, H- α), 3.39 and 3.29 (each 1H, m, H-1), 3.09-3.00 (10H, H-3, H-4, H-7, H-8 and H-10), 2.05 (2H, m, H-9), 1.90 (2H, m, H-2), 1.83-1.71 (8H, br m, H-5, H-6 and $4 \times cHex-H_{eq}$), 1.70-1.60 (3H, br m, $cHex-H_{eq}$ and H- β), 1.43 (1H, m, H- γ), 1.34-1.16 (3H, m, $cHex-H_{ax}$), 1.05-0.92 (2H, br m, $cHex-H_{ax}$). ^{13}C NMR (150 MHz, CD_3OD): δ 176.7, 168.8, 142.3, 136.1, 131.1, 130.1 (2C), 128.9 (2C), 121.4, 53.5, 48.3, 48.1, 46.1, 45.9, 40.3, 37.8, 36.7, 35.5, 34.9, 33.4, 27.6, 27.5, 27.4, 27.2, 25.4, 24.3 (2C).

Preparation of *Xenopus* oocytes and injection of cRNA. Oocytes isolated from mature female *Xenopus laevis* were supplied by the European Xenopus Resource Centre, University of Portsmouth, UK. Oocytes were treated with collagenase (0.5 mg/mL, Sigma type 1A) in Ca^{2+} -free solution (96 mM NaCl, 2 mM KCl, 1 mM $MgCl_2$, 5 mM HEPES, 2.5 mM sodium pyruvate, 100 U/mL penicillin, 0.1 mg/mL streptomycin, pH 7.5) with shaking at 19°C to separate individual oocytes from the connective tissue and to remove the follicular layer surrounding the cells. After separation, oocytes were washed 7 times with modified Barth's solution (96 mM NaCl, 2 mM KCl, 1.8 mM $CaCl_2$, 1 mM $MgCl_2$, 5 mM HEPES, 2.5 mM sodium pyruvate, 0.5 mM theophylline, 50 μ g/mL gentamicin, pH 7.5) and kept at 19°C in the same solution.

Healthy oocytes were injected with cRNA by using a Nanoliter Injector (World Precision Instruments, USA). Mixtures of nAChR subunit cRNAs were injected with a 1:1 ratio of α : β subunit at 200 ng/ μ L. Each oocyte was injected with 50 nL of RNA solution. Injected oocytes

were kept in Barth's solution at 19°C for two or three days to allow for expression of nAChRs. During this time oocytes were regularly inspected to remove unhealthy ones.

Electrophysiology. Electrophysiological recordings were obtained from nAChR-expressing oocytes by the two-electrode voltage clamp (TEVC) method, using a Geneclamp 500 voltage clamp amplifier (Axon instruments, USA). Oocytes were placed in a perfusion chamber by using a plastic Pasteur pipette and perfused (~5 mL/min) with fresh Frog Ringer solution (96 mM NaCl, 2 mM KCl, 1.8 mM CaCl₂ and 5 mM HEPES, pH 7.5). Microelectrodes were pulled from borosilicate glass capillaries (Harvard GC150TF-10) using a programmable micropipette puller (Sutter P97, USA), such that they had a resistance of between 0.5 and 2.5 MΩ when filled with 3 M KCl. Oocytes were voltage-clamped at a holding potential (V_H) of -100 mV. ACh was consistently used as the agonist, and it was applied at a fixed concentration without or together with variable concentrations of each of the PhTX analogues using an 8-channel perfusion system (Automate, USA) for 1 min to allow for equilibration of the current. Output from the amplifier was transferred to a PC via a digidata 1200 digital interface (Axon Instruments, USA) by using WinEDR v3.2.6 Software (Dr John Dempster, University of Strathclyde, UK).

Data analysis. WinEDR was used to measure the current amplitude of responses to ACh at the end of the one-minute application (i.e., "late" current) in order to allow for equilibration of the inhibitory effect, and hence to achieve improved comparison of the effect of test compounds. Currents in the presence of each concentration of each PhTX analogue were normalised as percentage of the control response (i.e., to ACh alone), and subsequently these were plotted against PhTX concentration. Graphpad Prism 7 was used for data analysis, graph plotting, and curve fitting. All plotted data points are the mean ± SEM, obtained from analysis of 4-20 oocytes. Concentration-inhibition curves were used to estimate IC₅₀ values by using the following equation (where nH is the Hill slope):

$$\text{Percentage of control response} = \frac{100\%}{1 + 10^{(\text{Log}[PhTX] - \text{Log}IC_{50})nH}} \quad (\text{Eq. 1})$$

IC₅₀ values were compared for significant differences by using an extra sum of squares F-test in Graphpad Prism 7.

Associated Content

Supporting Information: p. S2: Characterization of PhTX analogues; Molecular formula strings file (Kachel et al_mfs file.csv).

Author information

Corresponding Author: ian.mellor@nottingham.ac.uk

Present Address: Hamid S. Kachel, School of Life Science, Biology Department, University of Zakho, Duhok, Kurdistan Region, Iraq.

Author Contributions: HSK carried out the experimental work; IRM and HF designed the study; HSK and IRM analysed the data; IRM, HSK and HF wrote the manuscript.

Funding: The authors would like to acknowledge the financial support of the Ministry of Higher Education and Scientific Research of Kurdistan Regional Government (KRG) through their Human Capacity Developing Program (HCDP) to HSK. NMR equipment used in this work was purchased via grant #10-085264 from The Danish Research Council for Independent Research | Nature and Universe.

Notes

The authors declare no competing financial interest.

Acknowledgement

We acknowledge Birgitte Simonsen for purification of polyamine toxins and Uraivan N. Adamsen for mass spectrometric analysis of the compounds.

Abbreviations: ACh, acetylcholine; AMPA, α -amino-3-hydroxy-5-methyl-4-isoxazolepropionic acid; Boc; *tert*-butyloxycarbonyl; cBu, cyclobutyl; Cha, cyclohexylalanine; cHep, cycloheptyl; cHex, cyclohexyl; cPent, cyclopentyl; DIC, diisopropylcarbodiimide; Fmoc, fluoren-9-yl-methyloxycarbonyl; HOBt, 1-hydroxybenzotriazol; IC₅₀, concentration that results in 50% inhibition of the maximal response; iGluR, ionotropic glutamate receptor; nAChR, nicotinic acetylcholine receptor; NMDA, *N*-methyl-D-aspartate; PhTX, philanthotoxin; SPS, solid-phase synthesis; Teoc, 2-(trimethylsilyl)ethyloxycarbonyl; TEVC, two-electrode voltage clamp.

References

- (1) Eldefrawi, A. T.; Eldefrawi, M. E.; Konno, K.; Mansour, N. A.; Nakanishi, K.; Oltz, E.; Usherwood, P. N. Structure and synthesis of a potent glutamate receptor antagonist in wasp venom. *Proc. Natl. Acad. Sci. U. S. A.* **1988**, *85*, 4910-4913.
- (2) Piek, T. delta-Philanthotoxin, a semi-irreversible blocker of ion-channels. *Comp Biochem. Physiol. C* **1982**, *72*, 311-315.
- (3) Bähring, R.; Mayer, M. L. An analysis of philanthotoxin block for recombinant rat GluR6(Q) glutamate receptor channels. *J. Physiol.* **1998**, *509 (Pt 3)*, 635-650.
- (4) Mellor, I. R.; Brier, T. J.; Pluteanu, F.; Stromgaard, K.; Saghyan, A.; Eldursi, N.; Brierley, M. J.; Andersen, K.; Jaroszewski, J. W.; Krogsgaard-Larsen, P.; Usherwood, P. N. Modification of the philanthotoxin-343 polyamine moiety results in different structure-activity profiles at muscle nicotinic ACh, NMDA and AMPA receptors. *Neuropharmacol.* **2003**, *44*, 70-80.
- (5) Bixel, M. G.; Krauss, M.; Liu, Y.; Bolognesi, M. L.; Rosini, M.; Mellor, I. S.; Usherwood, P. N.; Melchiorre, C.; Nakanishi, K.; Hucho, F. Structure-activity relationship and site of binding of polyamine derivatives at the nicotinic acetylcholine receptor. *Eur. J. Biochem.* **2000**, *267*, 110-120.
- (6) Brier, T. J.; Mellor, I. R.; Tikhonov, D. B.; Neagoe, I.; Shao, Z.; Brierley, M. J.; Stromgaard, K.; Jaroszewski, J. W.; Krogsgaard-Larsen, P.; Usherwood, P. N. Contrasting actions of philanthotoxin-343 and philanthotoxin-(12) on human muscle nicotinic acetylcholine receptors. *Mol. Pharmacol.* **2003**, *64*, 954-964.
- (7) Kachel, H. S.; Patel, R. N.; Franzyk, H.; Mellor, I. R. Block of nicotinic acetylcholine receptors by philanthotoxins is strongly dependent on their subunit composition. *Sci. Rep.* **2016**, *6*, 38116.

- (8) Liu, M.; Nakazawa, K.; Inoue, K.; Ohno, Y. Potent and voltage-dependent block by philanthotoxin-343 of neuronal nicotinic receptor/channels in PC12 cells. *Br. J. Pharmacol.* **1997**, *122*, 379-385.
- (9) Mellor, I. R.; Usherwood, P. N. Targeting ionotropic receptors with polyamine-containing toxins. *Toxicon* **2004**, *43*, 493-508.
- (10) Tikhonov, D. B.; Mellor, I. R.; Usherwood, P. N. Modeling noncompetitive antagonism of a nicotinic acetylcholine receptor. *Biophys. J.* **2004**, *87*, 159-170.
- (11) Brackley, P. T.; Bell, D. R.; Choi, S. K.; Nakanishi, K.; Usherwood, P. N. Selective antagonism of native and cloned kainate and NMDA receptors by polyamine-containing toxins. *J. Pharmacol. Exp. Ther.* **1993**, *266*, 1573-1580.
- (12) Olsen, C. A.; Mellor, I. R.; Wellendorph, P.; Usherwood, P. N.; Witt, M.; Franzyk, H.; Jaroszewski, J. W. Tuning wasp toxin structure for nicotinic receptor antagonism: cyclohexylalanine-containing analogues as potent and voltage-dependent blockers. *ChemMedChem* **2006**, *1*, 303-305.
- (13) McCallum, S. E.; Cowe, M. A.; Lewis, S. W.; Glick, S. D. alpha 3 beta 4 nicotinic acetylcholine receptors in the medial habenula modulate the mesolimbic dopaminergic response to acute nicotine in vivo. *Neuropharmacol.* **2012**, *63*, 434-440.
- (14) Glick, S. D.; Maisonneuve, I. M.; Kitchen, B. A. Modulation of nicotine self-administration in rats by combination therapy with agents blocking alpha 3 beta 4 nicotinic receptors. *Eur. J. Pharmacol.* **2002**, *448*, 185-191.
- (15) Toll, L.; Zaveri, N. T.; Polgar, W. E.; Jiang, F. M.; Khroyan, T. V.; Zhou, W.; Xie, X. M.; Stauber, G. B.; Costello, M. R.; Leslie, F. M. AT-1001: A High Affinity and Selective alpha 3 beta 4 Nicotinic Acetylcholine Receptor Antagonist Blocks Nicotine Self-Administration in Rats. *Neuropsychopharmacol.* **2012**, *37*, 1367-1376.
- (16) Frolund, S.; Bella, A.; Kristensen, A. S.; Ziegler, H. L.; Witt, M.; Olsen, C. A.; Stromgaard, K.; Franzyk, H.; Jaroszewski, J. W. Assessment of structurally diverse philanthotoxin analogues for inhibitory activity on ionotropic glutamate receptor subtypes: discovery of nanomolar, nonselective, and use-dependent antagonists. *J. Med. Chem.* **2010**, *53*, 7441-7451.
- (17) Jorgensen, M. R.; Jaroszewski, J. W.; Witt, M.; Franzyk, H. On-resin carboxy group activation of omega-amino acids in solid-phase synthesis of philanthotoxin analogues. *Synthesis-Stuttgart* **2005**, 2687-2694.
- (18) Chang, Y. P.; Banerjee, J.; Dowell, C.; Wu, J.; Gyanda, R.; Houghten, R. A.; Toll, L.; McIntosh, J. M.; Armishaw, C. J. Discovery of a potent and selective alpha3beta4 nicotinic acetylcholine receptor antagonist from an alpha-conotoxin synthetic combinatorial library. *J. Med. Chem.* **2014**, *57*, 3511-3521.
- (19) Anis, N.; Sherby, S.; Goodnow, R., Jr.; Niwa, M.; Konno, K.; Kallimopoulos, T.; Bukownik, R.; Nakanishi, K.; Usherwood, P.; Eldefrawi, A.; Eldefrawi, M. Structure-activity relationships of philanthotoxin analogs and polyamines on N-methyl-D-aspartate and nicotinic acetylcholine receptors. *J. Pharmacol. Exp. Ther.* **1990**, *254*, 764-773.

- (20) Franzyk, H.; Grzeskowiak, J. W.; Tikhonov, D. B.; Jaroszewski, J. W.; Mellor, I. R. The effects of conformational constraints in the polyamine moiety of philanthotoxins on AMPAR inhibition. *ChemMedChem* **2014**, *9*, 1725-1731.
- (21) Wellendorph, P.; Jaroszewski, J. W.; Hansen, S. H.; Franzyk, H. A sequential high-yielding large-scale solution-method for synthesis of philanthotoxin analogues. *Eur. J. Med. Chem.* **2003**, *38*, 117-122.
- (22) Jorgensen, M. R.; Olsen, C. A.; Mellor, I. R.; Usherwood, P. N.; Witt, M.; Franzyk, H.; Jaroszewski, J. W. The effects of conformational constraints and steric bulk in the amino acid moiety of philanthotoxins on AMPAR antagonism. *J. Med. Chem.* **2005**, *48*, 56-70.

TOC graphic

